


National Spherical Torus eXperiment - Upgrade

NSTX-U

Inner PF Coil Thermal Analysis

NSTXU-CALC-133-27 - Rev 0
March 14, 2018

Yuhu Zhai
Digitally signed by Yuhu Zhai
Date: 2018.03.29 08:42:20 -04'00'

Yuhu Zhai
Prepared By

Art Brooks
Digitally signed by Art Brooks
Date: 2018.03.29 07:47:42 -04'00'

Art Brooks
Reviewed By

Michael Kalish
Digitally signed by Michael Kalish
Date: 2018.03.29 07:51:09 -04'00'

Mike Kalish
Approved By – Responsible Engineer

Steve Raftopoulos
Digitally signed by Steve Raftopoulos
Date: 2018.03.29 13:41:27 -04'00'

NSTX-U CALCULATION

Record of Changes

Rev.	Date	Description of Changes	Revised by
0	3/14/18	Initial Release	Yuhu Zhai

NSTX-U Calculation Form

Purpose of Calculation: The NSTX-U inner PF coils are water-cooled copper solenoids fabricated from rectangular or square shaped conductors with embedded central cooling channels. The inner PF coils, consist of three upper and lower coil pairs, denoted PF-1a, PF-1b and PF-1c, are energized up to 20 kA for about 1-2 seconds during plasma operations and then cooled down with 12 ^{0}C cold water once every 1200 seconds. The inner PFs are designed to have 20,000 pulse cycles in which conductors for all six coils will experience a thermal fatigue stress during machine operations. This calculation is to determine the maximum temperatures and transient cool down times of the conductor and the insulations when coils are pulsed, and during cool down when coils are de-energized. The 2D transient thermal analysis is followed by a time dependent structural analysis of the coil winding pack so to evaluate thermal stresses and strains in the conductor and insulation with respect to the structural design limit. When pulsed, coils are heated up to the maximum temperature almost instantaneously and uniformly on the conductor but a normal tensile strain in the turn insulation is induced as a result of large temperature gradient between adjacent turns at the coil inlet (the most outer layer of winding pack) during cool down periods. The results show that conductor stresses meet the design allowable, but the level of insulation tensile strain is sensitive to the insulation elastic modulus. Therefore, maintaining a higher level insulation elastic modulus is important to minimize its impact to its tensile strain that may degrade the electrical performance and compromise coil structural integrity. The thermal analysis results also show that the inner PF coil design meets the cool down and repetition cycle requirements per NSTX-U General Requirements Document [1] and the System Requirements Document for Magnet Systems [2].

References:

[1] NSTX-U-RQMT-GRD-001-00 General Requirements Document, S. Gerhardt, December, 2017

[2] NSTX-U-RQMT-SRD-002-00 System Requirements Document Magnet Systems, S. Gerhardt, December, 2017.

[3] Inner PF Coil Design Parameters, M. Kalish, February, 2018.

[4] NSTX-CRIT-0001-02 Structural Design Criteria, I. Zatz, January, 2016

[5] NSTX-U-SPEC-MAG-001-2 Specification for Inner PF Coil Conductor, M. Kalish, November, 2017

[6] PF1A Conductor Dimension and Cooling Hole Size, NSTX-U engineering memo, MAG-171003-YZ-02, Y. Zhai, December, 2017.

[7] FCOOL thermal code, A. Brooks, Private communications.

[8] Inner PF coil fatigue and fracture mechanics calculation, NSTX-U_CALC-CC-#-Rev 0, January, 2018.

[9] Inner-PF Coil Interfaces to Supports Designs and Cooling Systems, NSTX-U_RQMT-RD-012-00, S. Gerhardt, March, 2018.

[10] Material Properties for Inner PF Coil FDR, MAG-180306-YZ-01, Y. Zhai, March 12, 2018.

Assumptions:

The transient thermal analysis performed here is based on the updated inner PF coil design parameters including changes made to the PF-1a conductor size after inner PF PDR [3], following the new NSTX-U physics requirements for the inner PF magnet system [2]. A 2D axis-symmetric model for each of the PF-1a, 1b and 1c coils is generated for the transient thermal analysis, followed by time-dependent structural analysis on each of the PFs. This report summarizes the results from the 2D thermal and structural calculations under thermal loads when coils are pulsed and during cool down for the new design of the inner PF coils.

Calculation:

Contents

1. Executive Summary

The inner PF coils for the NSTX-U are installed to provide the poloidal field shaping and better controlling of plasma in the diverter region during machine operations. The inner PFs, fabricated from rectangular or square shape copper conductors with embedded central cooling channels, are designed to have 20,000 pulse cycles over the machine lifetime as defined in the NSTX-U General Requirement Document [1]. The key design requirements include 1) the repetition period of operations shall not exceed 1200 seconds, 2) the maximum temperature for operations shall be below 100 ^{0}C. To this end, 1D and 2D fluid-structural coupled thermal analyses were performed based on the FCOOL [7] and axis-symmetric models of PF-1a, PF-1b and PF-1c coil cross-sections to validate the coil design [3]. The thermal results show that maximum temperatures on the conductor when pulsed are 58, 90 and 48 ^{0}C for PF-1a, -1b and -1c coils respectively. While all coils meet the 1200 seconds cool down requirement, there is a little bit thermal ratcheting for PF-1a coil as a result of ~5% conductor size reduction [6]. Moreover, PF-1b coils cool down fairly quickly in the first 3-5 minutes, while PF-1a and -1c coils cool down more gradually as a result of larger winding pack size or longer pulses. According to the NSTX-U structural design criteria [4], a fatigue strength evaluation is required for all structural components including the conductors and insulations, with undetectable flaws that are either cycled over 10,000 times during their operational lives or are exposed to cyclic peak stresses exceeding yield stress. A fatigue strength evaluation is performed for the 2D coil winding pack. As an important part of the coil design validation process, the fatigue strength evaluation includes meeting the requirements of either the design Stress-N (S-N) fatigue curve derived from material test data, or the crack growth limitation for the 20,000 cycles.

2. Inner PF Coil Design

The coil geometry and conductor dimension in the transient thermal analysis models are taken from the latest Kalish Coil Design Parameter data sheet [3]. To ensure a self-consistent coil alignment with consideration of assembly and positional tolerances of components, the PF-1a conductor width was reduced by 1 mm since inner PF PDR so to increase the Center Stack Casing inner bore size by 8 mm (4 mm on each side), and the cooling hole size for PF-1a is reduced from 0.225” to 0.185” accordingly so to maintain the same width from hole edges to conductor outer edges for the fatigue crack propagation of 1mm size minimum detectable flaws [8]. The Equivalent Square Wave (ESW) time for PF-1a is reduced accordingly from 2.1 s to 1.9 s so to maintain the same maximum temperature with the proposed conductor modification [2, 6]. Table1 listed the latest physics requirements for the inner PF coil design.

Table 1 – Inner PF Physics Requirements

	PF-1a	PF-1b	PF-1c
No. of turns	61	20	16
Max current (kA)	19.67	20	20.25
ESW time (s)	1.9	1.0	1.4

Tables 2-3 listed the coil design parameters and the inner PF conductor dimensions [3], which are used as the input to create the 2D axis-symmetric thermal analysis models. Figure 1 presents the inner PF coils in the polar region of NSTX-U, and the 2D cross section of the PF-1b used in the thermal analysis model.

Table 2 – Inner PF Coil Design Parameters

		MK PF Coil Sizing 02-01-18					
		PF1A (")	**PF1B (")**	**PF1C (")**	**PF1A (mm)**	**PF1B (mm)**	**PF1C**
R center	r_0=	**12.81**	15.44	21.85	325.4	392.2	555.0
Z center	z_0=	62.62	71.03	71.4	1590.5	1804.2	1813.6
Coil ID	ID=	**23.03**	29.32	41.66	585.0	744.7	1058.2
Coil OD	OD=	28.21	32.44	45.74	716.5	824.0	1161.8
Width	w=	**2.59**	1.56	2.04	58.1	32.0	44.1
Height	h=	18.44	7.17	6.94	460.7	174.4	168.6

Table 3 – Inner PF Conductor Dimensions

Conductor		PF1A (")	PF1B	PF1C	PF1A (mm)	PF1B	PF1C
Width		**0.481**	0.54	0.78	12.2174	13.716	19.812
Height		0.98	0.5	0.61	24.892	12.7	15.494
hole		**0.185**	0.146	0.146	4.699	3.7084	3.7084

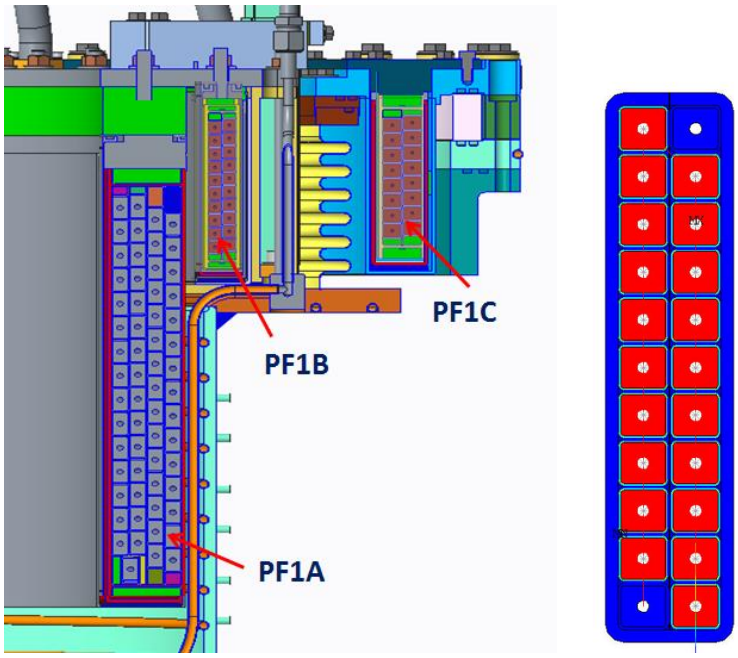

Figure 1 Inner PFs in Polar Region (left) and 2D Analysis Model of PF-1b (right)

3. Structural Design Limits

According to [4], fatigue S-N fatigue curves shall be obtained based on the uniaxial strain cycling tests at service temperatures and at various R ratios. S-N fatigue curves shall be developed for both the base metal and for braze joints in the coil lead region.

a. The conductor static stress design limit is derived from the minimum yield strength given in the specifications for the inner PF conductors
b. The fatigue limit for copper is derived from the copper fatigue S-N curve

Figure 2 presents the stress categorization from the structural design criteria, and the static and fatigue fatigue S-N curve from copper test data available from a number of references. For S-N fatigue evaluation, the more strict criteria of 2 on stress and 20 on life must be met. For the fracture mechanics evaluation, a factor of 2 on minimum detectable flaw size, 1.5 on fracture toughness, and 2 on life must be met. The measured NSTX OH conductor braze joint fatigue life is also included in the evaluation, along with the published S-N data for comparison.

- *NSTX-U Structural Design Criteria*
  - Coils are evaluated by comparing Tresca stress to design limits
  - Main loads include EM (96 EQ) and Thermal during cool down

Stress Category	Parameters	Stress Intensity Limits
General primary membrane	P_m	$k\ S_m$
Local primary membrane	P_L	$1.5\ k\ S_m$
Primary membrane plus bending	$(P_m + P_b)$ or $(P_L + P_b)$:	$1.5\ k\ S_m$
Primary plus secondary	$(P_m + P_b + Q)$ or $(P_L + P_b + Q)$	$3\ S_m$

- *S_m - design stress limit, based on load cases*
  - *k*-factor – Normal operation *k = 1.0*
  - Anticipated events *k = 1.1*
  - Unlikely events: *k = 1.2*

- *Static*
  - S_m is the smaller of $^2/_3\ \sigma_y$ or $^1/_2\ \sigma_u$ at the service temperature

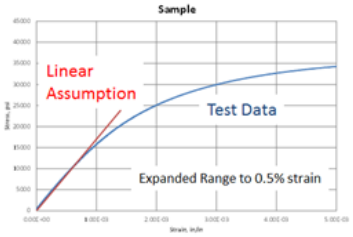

σ_y (MPa)	σ_u	S_m	$1.5*S_m$	$3*S_m$	Temperature
103	221	69	103	207	20 C
93	198	62	93	186	100 C

- *Fatigue* - Total cycles of 20,000 – *NSTX CSU Pulse Spectrum*

Criteria	Stress Level ant Type	Actual
SN 2 on stress	112 MPa (Tresca)	142
SN 20 on life	180 (Tresca)	142
Fracture Mechanics with a flaw size less than .7mm 1.5 on KIc and 2 on Cycles	140 MPa (Max Principal or Hoop)	101
4 on cycles	125 MPa (Max Principal or Hoop)	101

Conductor Fatigue and Fracture Mechanics Analyses

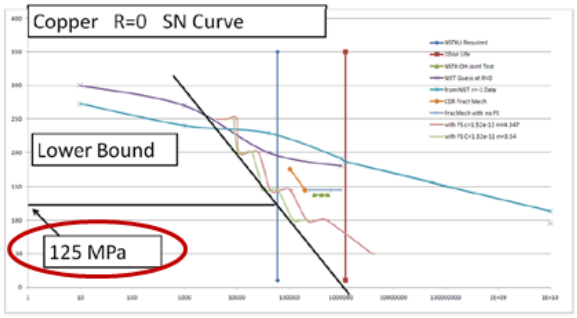

Figure 2 SN and Fracture Mechanics Fatigue Life

Figure 2 Structural Design Criteria and Conductor Static and Fatigue Limits

4. Transient Thermal Analysis

Two-dimensional axis-symmetric transient thermal analysis models were developed for each of the PF1-a, PF1-b and PF1-c coils as shown in Figure 2 below. The 2D thermal models include conductors with 1 mm corner radius, turn-to-turn and layer insulations, as well as the ground wrap insulations. The cooling layout has been optimized to reduce hoop stresses such that the 12 ^{0}C cold water (cooling inlet) is always in the outer layer of the coil winding pack, while the hot end outlet is always on the most inner layer of the winding pack. Figure 3 presents the cooling layout with inlet (the most outer layer) and the outlet (the most inner layer) of PF-1a and -1c in the analysis model, as well as the typical mesh with fluid116 and surf151 elements used for the 2D thermal analysis.

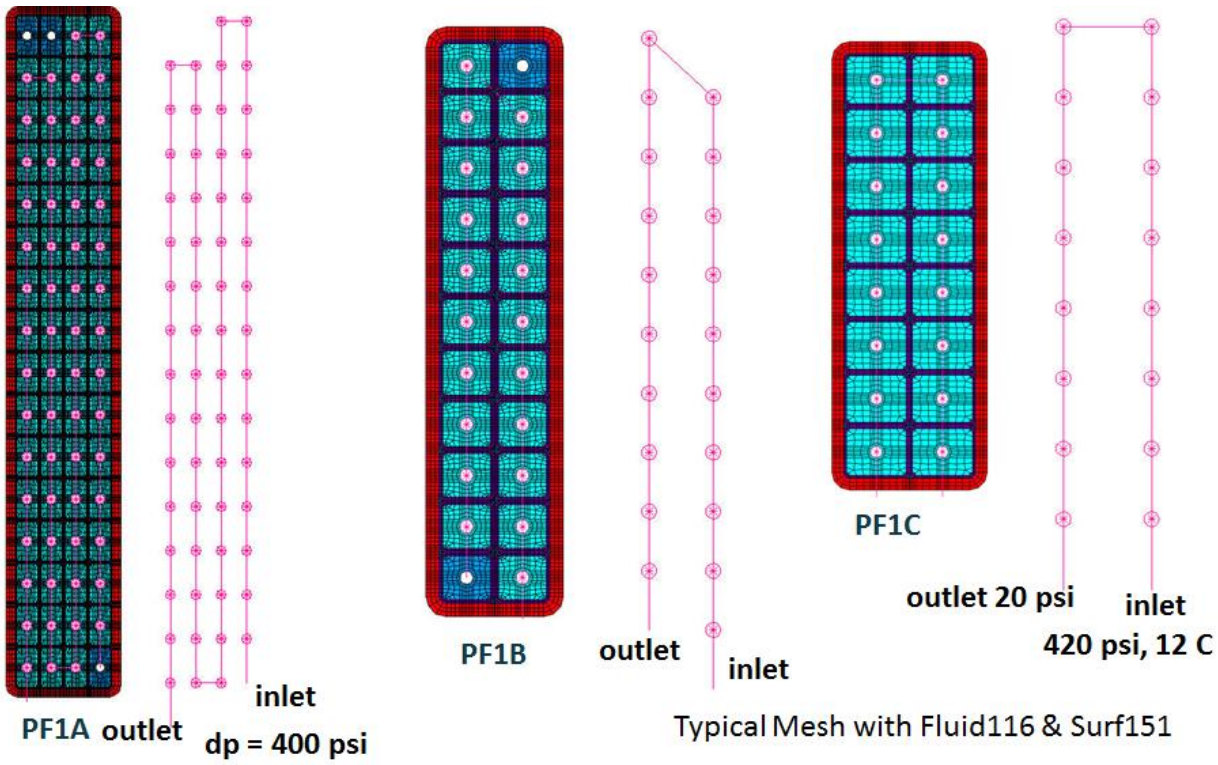

Figure 3 Transient Thermal Analysis Models for PF-1a and PF-1c

Table 4 – Inner PF Cooling Parameters

	PF-1a	PF-1b	PF-1c
Inlet temperature (^{0}C)	12	12	12
Pressure drop (psi)	400	400	400
Outlet pressure (psi)	20	20	20
flow velocity (m/s)	2.5	3.3	3.2

The cooling water flow rates are selected based on the available pressure drops given in the inner-PF coil interface document [7]. The flow varies with temperature due to

large variation in viscosity while the pump is assumed to deliver a constant pressure and not limited by the flow. Other assumptions for the 2D analysis include 1) insulations are bonded to the conductors without delamination and linear elastic behavior is used for copper without yielding; 2) no heat conduction between coil winding pack (warm) and its support structure (cold); 3) isotropic properties of the copper conductor and orthotropic mechanical properties of insulations are used as described in reference [8].

A sensitivity study has been performed to quantify the impact due to uncertainty of insulation elastic modulus to the conductor stress and insulation tensile strain during cool down. The maximum tensile strain occurs at about the first 3-5 minutes during cool down. The vertical constraint of the coil winding pack is also introduced into the thermal model to limit the insulation normal strain for PF-1a and PF-1b coils. The coil support design provides new features with new level of pre-loads for the PF-1a and PF-1b coils. The pre-loads (100 kip for PF-1a and 60 kip for PF-1b coils) provided from coil support structures is defined in the inner-PF coil interface document [9].

Two groups of insulation material properties are used for the sensitivity study of the inner PF thermal performance. Both high end and low end of the insulation composite elastic moduli listed in Table 3 and Table 7 of reference [10] are used for the sensitivity study.

5. Thermal Results

When inner PFs are energized, the coil conductor is pulsed up to ~20 kA for about 1-2 seconds. Both conductor and insulation will experience the thermal fatigue stress and strain, but the thermal stress during cool down dominates the fatigue evaluation for the conductor and stress due to Lorentz loads dominates fatigue evaluation for current lead sections (lead in and lead out) at coil terminals. During normal operation, the equivalent square wave (ESW) time of PF-1a, -1b and -1c coils is 1.9, 1.0 and 1.4 seconds respectively as shown in Table 1.

Maximum Conductor Temperature and Coil Free Thermal Expansion

The transient temperatures at the conductor outlets (the most inner layer) during cool down for the inner PFs are shown in Figure 4. Although inner PF coils meet the cool down time requirements, the cool down of PF-1b is much faster than that of PF-1a and -1c. Figure 5 presents the temperature gradient at 84 s, 24 s, and 36 s of cool down in the 2D cross section of the PF-1a, PF-1b and PF-1c coils. The highest temperature gradient during cool down is in the PF-1b coils. Temperature distribution shown in Figure 5 clearly indicates a large temperature gradient is induced from the bottom to top turns in the inlet (the most outer layer). It is this large temperature gradient among adjacent turns that leads to the development of normal tensile strains in the turn

insulation. The peak thermal stresses in the PF winding pack are shown in Figures 8-10. Tresca stress or stress intensity is used for static evaluation and the maximum hoop stress is used for fatigue crack growth evaluation if the fatigue S-N curve cannot be satisfied. The transient thermal stresses including stress intensity and maximum hoop stress distribution in inner PFs are presented in the following section.

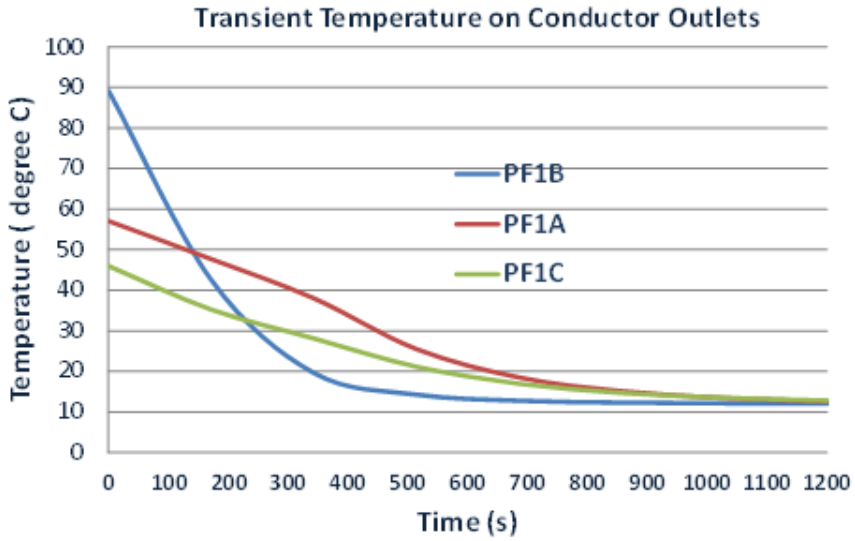

Figure 4 Transient temperatures on conductor outlet during cool down

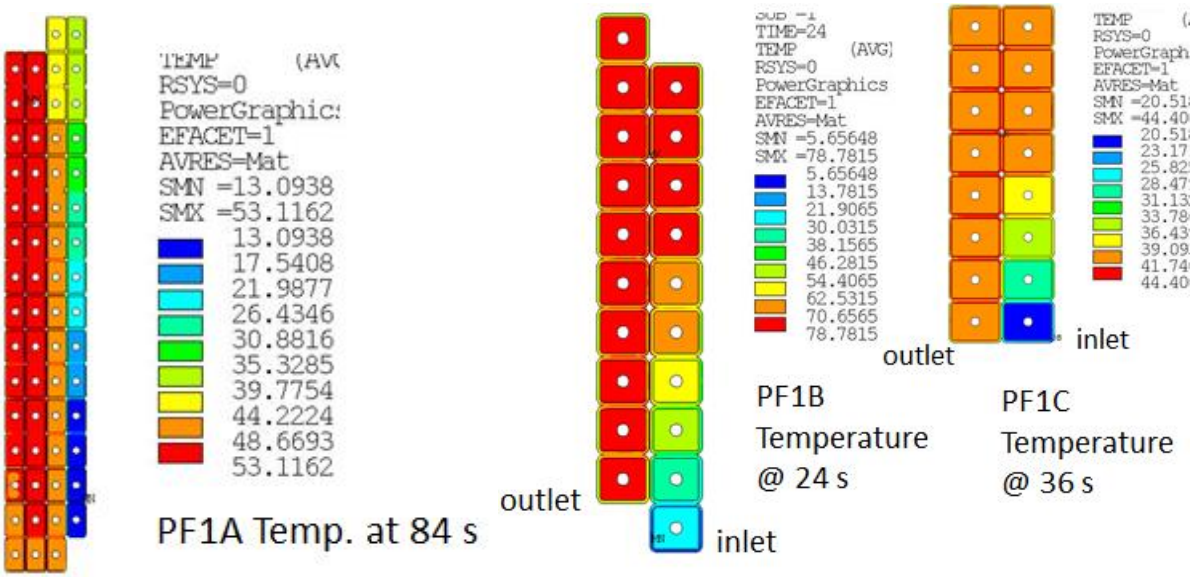

Figure 5 Temperature gradients evaluated for 3 PF coils. The highest gradient is in PF-1b during cool down

The conductor is hot (at its maximum temperature) at the end of pulses as shown in Figure 6. The free thermal expansion of coil winding pack is listed in Table 5. When pulsed, the inner PFs expand thermally only a fraction of a millimeter. The vertical

growth of coil pack is smaller than that of copper free growth due to constraints of insulations and ground wraps to the copper conductor.

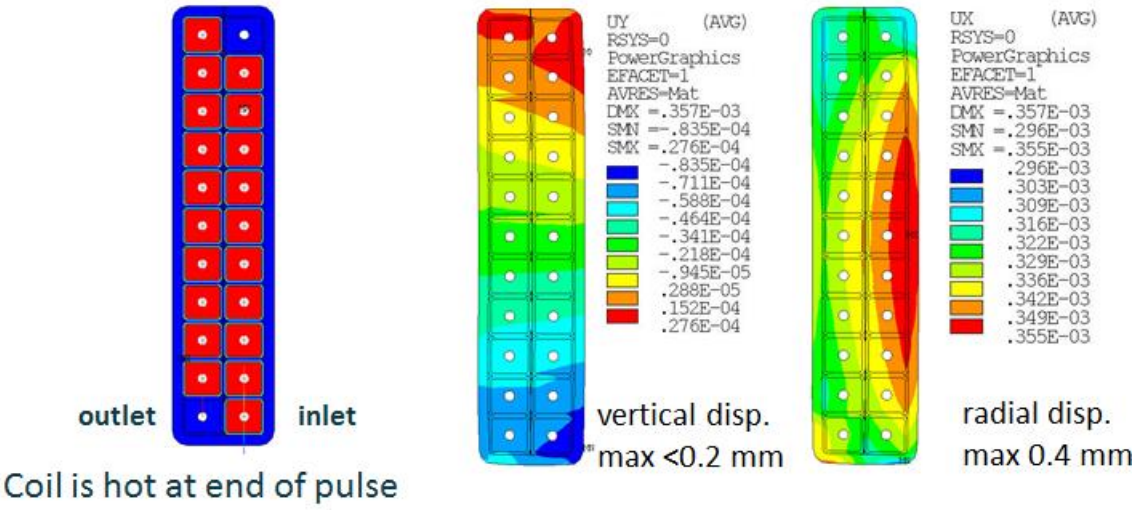

Figure 6 Temperature at end of pulse and maximum thermal expansion.

Table 5 – Inner PF Coil Free Thermal Expansion

	PF-1a	PF-1b	PF-1c
dT (^{0}C)	48	78	38
Cu vertical free growth (mm)	0.36	0.23	0.1
Vertical growth (mm)	0.171	0.117	0.04
Radial growth (mm)	0.154	0.355	0.15

More details of the transient cool down process for PF-1a, -1b and -1c coils are presented in Figure 7, where temperatures along the coil winding at various cool down times are shown in different colors. The results demonstrate that coil design meets the 1200 second cool down requirements. In addition, the PF-1b coils cool down much more quickly with >50 ^{0}C temperature drop during the first 3 minutes of the cool down. The PF-1a and -1c coils, on the other hand, cool down more slowly with only 10-15 ^{0}C temperature drops within the first 3 minutes. The total cool down time for the PF-1b coil is 1029 seconds, which is less than the 1200 second requirement. The maximum temperature on both PF-1b and -1c coils at the end of cool down time are slightly higher than 12 ^{0}C. For the PF-1a, however, there are a few degrees thermal ratcheting effect as a result of conductor size reduction as described in the last section of this report [6].

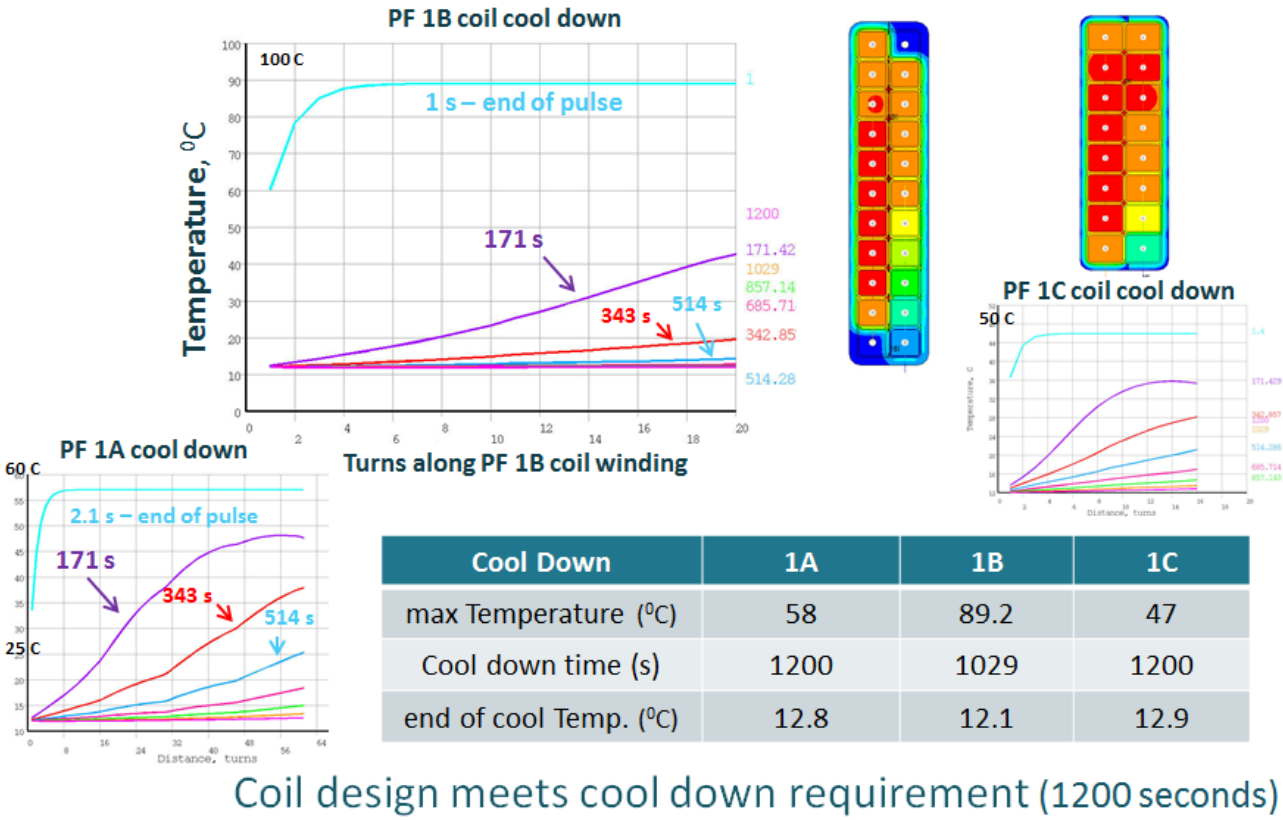

Cool Down	1A	1B	1C
max Temperature (0C)	58	89.2	47
Cool down time (s)	1200	1029	1200
end of cool Temp. (0C)	12.8	12.1	12.9

Coil design meets cool down requirement (1200 seconds)

Figure 7 Transient cool down temperature and temperature gradients.

Thermal Stresses in Conductors during Cool Down

Although stresses induced under thermal loads during cool down are secondary (self-limiting), a fatigue evaluation is still required for the inner PF coil conductor. Transient thermal stresses during cool down of the PF-1a, -1b and -1c coils are shown in Figures 8-10. The stress results are also summarized in Table 6. These results demonstrate that coil design meets the conductor static and fatigue requirements per NSTX-U structural design criteria [4]. As expected and consistent with the transient temperature distribution during cool down, the maximum conductor stress intensity occurs within the first 2-3 minutes during the cool down. The maximum stress intensity in PF-1a is below 100 MPa when the pre-load provided from the coil support structure is applied. The PF-1b and PF-1c coils, on the other hand, have lower static (stress intensity) and fatigue (hoop) stresses. The conductor stress meets allowable with less than 0.1% elastic strain on the conductor.

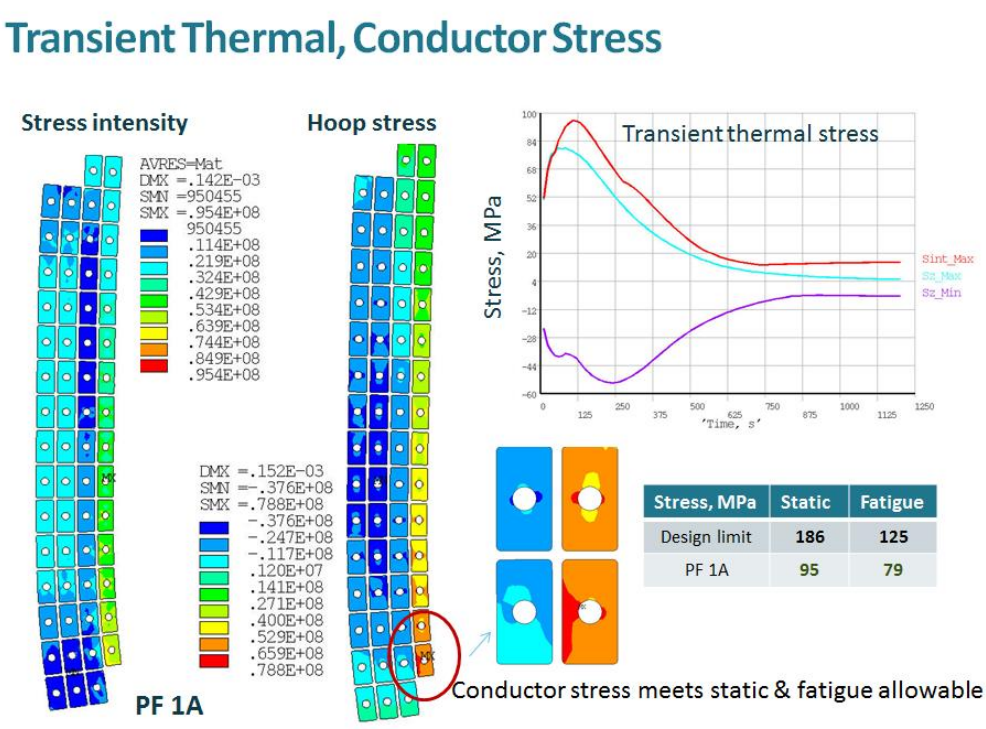

Figure 8 PF-1a conductor stresses during transient cool down

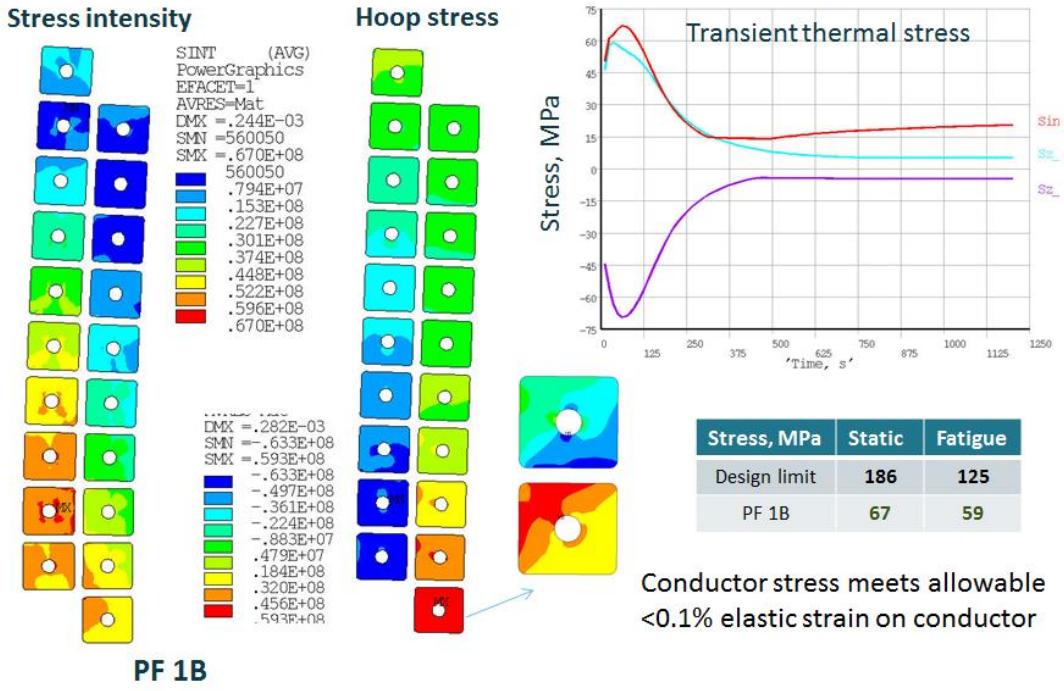

Figure 9 PF-1b conductor stresses during transient cool down

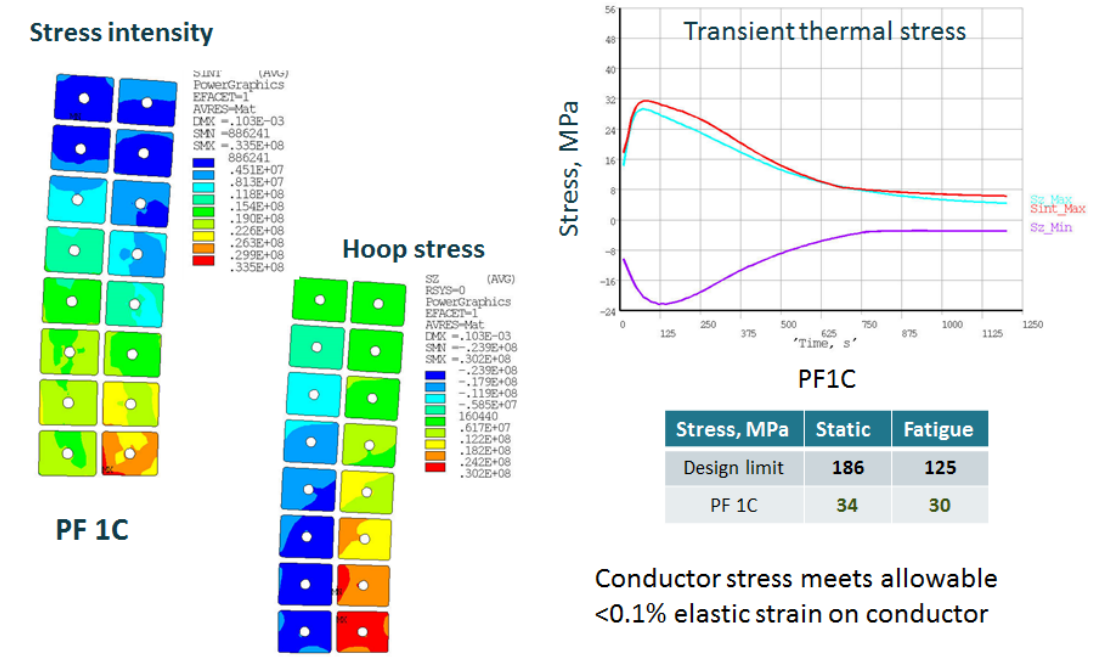

Figure 10 PF-1c conductor stresses during transient cool down

Table 6 – Summary of Conductor Thermal Stresses

Design Limit (MPa)		PF-1a	Pf-1b	PF-1c
Static	186	95	67	34
Fatigue	125	79	59	30

Thermal Stress and Strain in Coil Insulations

A critical issue with the coil insulation is the normal tensile strain induced in the turn insulations during cool down of the conductors where ~10-15 degrees of temperature gradient is developed between adjacent turns of the conductor in the cooling inlet layer, the most outer layer of the coil winding pack. Figures 11-13 present the transient normal tensile strain developed in the turn insulation during cool down if no preload is applied. The coil support design will provide 100 kip and 60 kip pre-loads for the PF-1a and PF-1b coils [7]. Figure 14 presents the reduced tensile strain in the turn insulation when pre-loads on the PF-1a and -1b coils are applied.

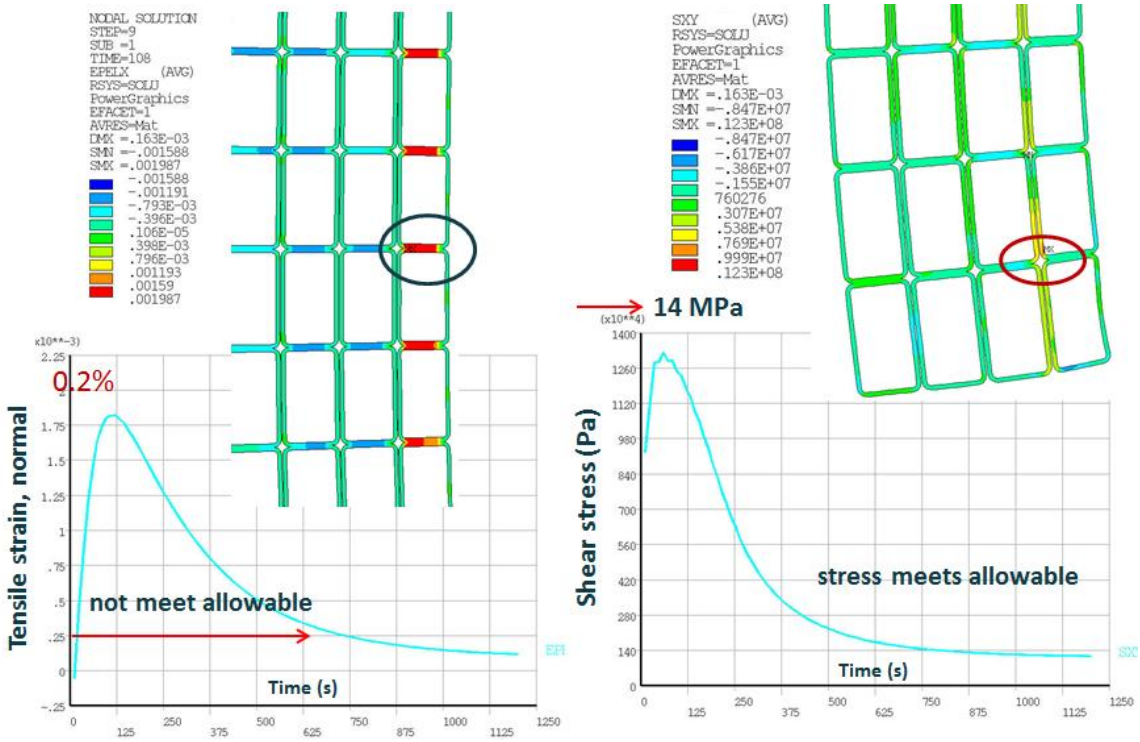

Figure 11 PF1a - Insulation normal tensile strain during transient cool down

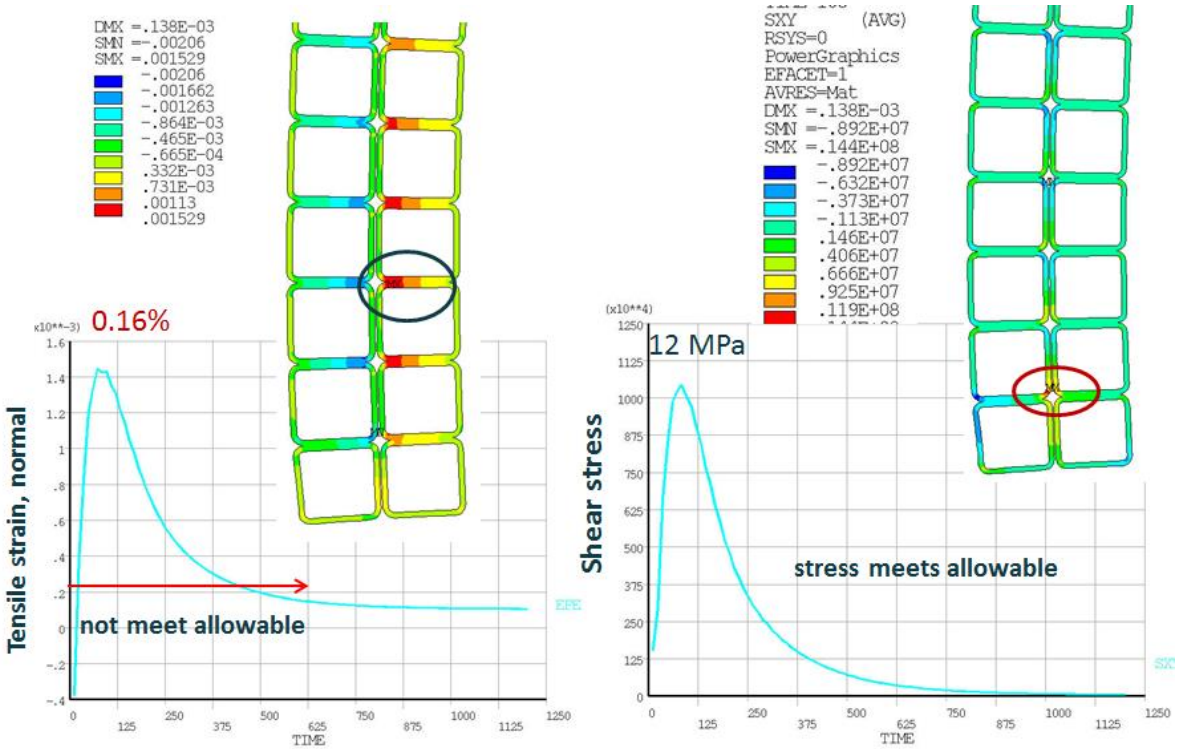

Figure 12 PF1b - Insulation normal tensile strain during transient cool down

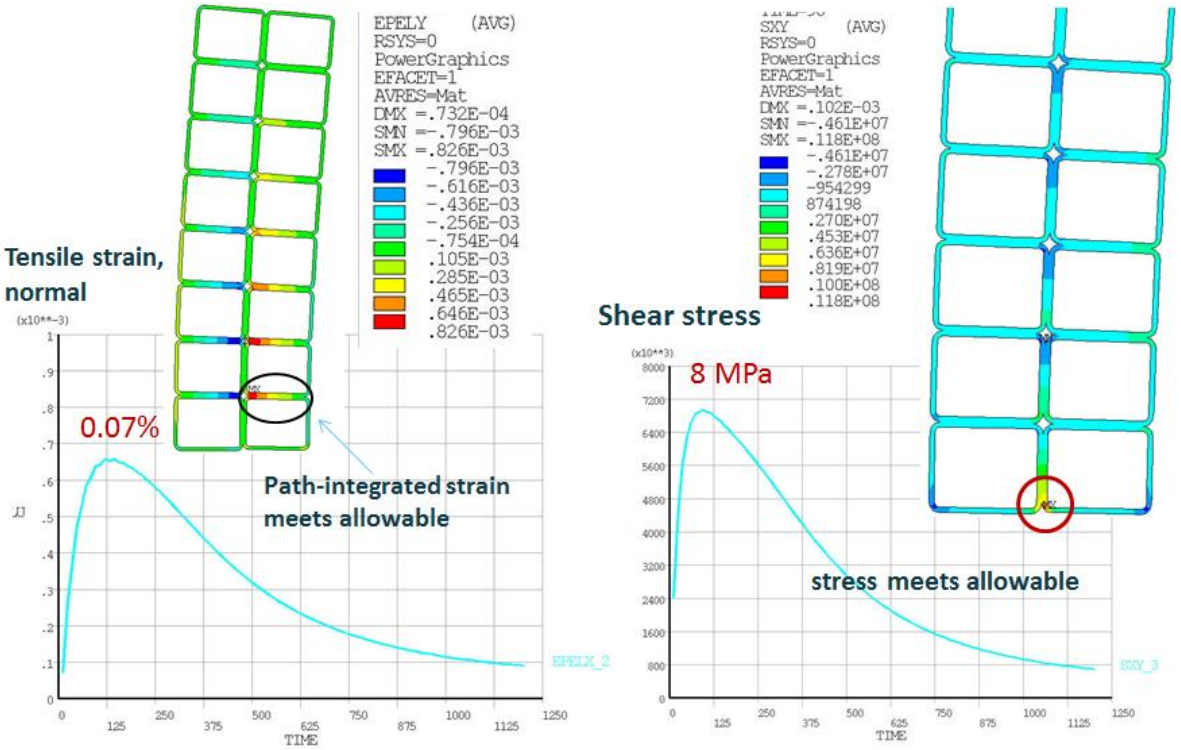

Figure 13 PF1c - Insulation normal tensile strain during transient cool down

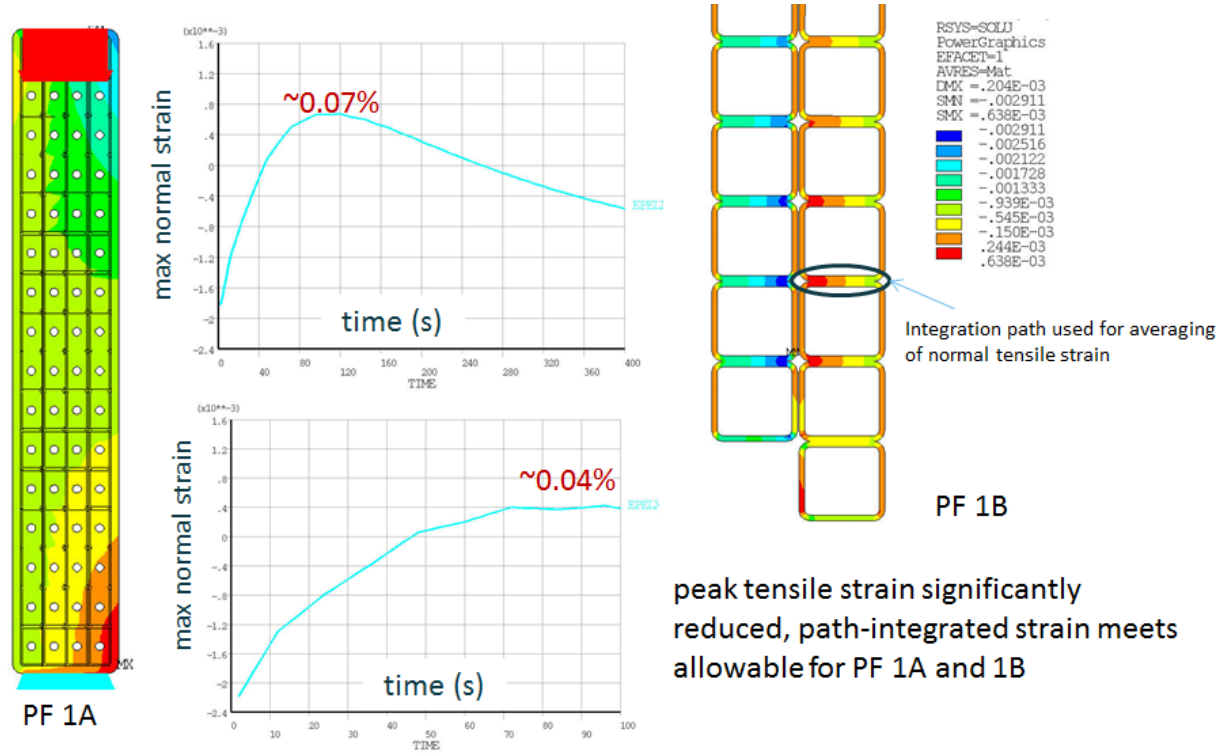

Figure 14 PF1a and 1b - Insulation normal tensile strain when pre-loaded on coils

Table 7 – Summary of Insulation Thermal Stress and Strain

	1A	1B	1C
shear stress (MPa)	12	14	12
Tensile strain – no preload (%)	0.2	0.16	0.07
Tensile strain w/ preload (%)	0.07	0.04	N/A

Sensitivity Study – Material properties on Insulation Strain

Due to uncertainty in insulation mechanical properties [8] such as the elastic modulus, the coefficient of thermal expansion, a sensitivity study was performed to quantify the impact of this uncertainty to the insulation strain level developed during cool down. To this end, a higher and lower end of compressive moduli (varying by a factor of 3) in turn insulations were used and results are presented here.

Table 8 – Insulation Properties Used for Sensitivity Study

Elastic properties	High modulus	Low modulus	unit
E_x	**12.5**	4.5	GPa
E_y	**25**	8.1	GPa
E_z	**25**	14.7	GPa
G_{xy}	4.7	1.88	GPa
G_{yz}	10.7	3.88	GPa
G_{xz}	4.7	1.88	GPa
v_{xy}	0.33	0.31	
v_{yz}	0.17	0.423	
v_{zx}	0.33	0.31	
α_x	25×10^{-6}	25×10^{-6}	$1/^0C$
α_y	10×10^{-6}	10×10^{-6}	$1/^0C$
α_z	10×10^{-6}	10×10^{-6}	$1/^0C$

Table 8 listed the insulation mechanical properties used for the sensitivity study. Lower elastic modulus in the insulation will result lower stresses in conductor and insulation but higher normal strains in the insulation. Although mass density and thermal conductivity of insulations can have a noticeable effect on the conductor stresses, the impact of insulation mechanical properties such as elastic modulus to the conductor stress and strain is very limited (~5%). The impact to the insulation strain, on the other hand, is much higher. Figures 15-16 present the maximum insulation tensile strain induced in the PF-1a and PF-1b coils (with and without pre-loads) using the insulation properties listed in the Table 8. Table 9 presents the impact of insulation properties to the conductor and insulation stress and strain, as well as interface pre-loads.

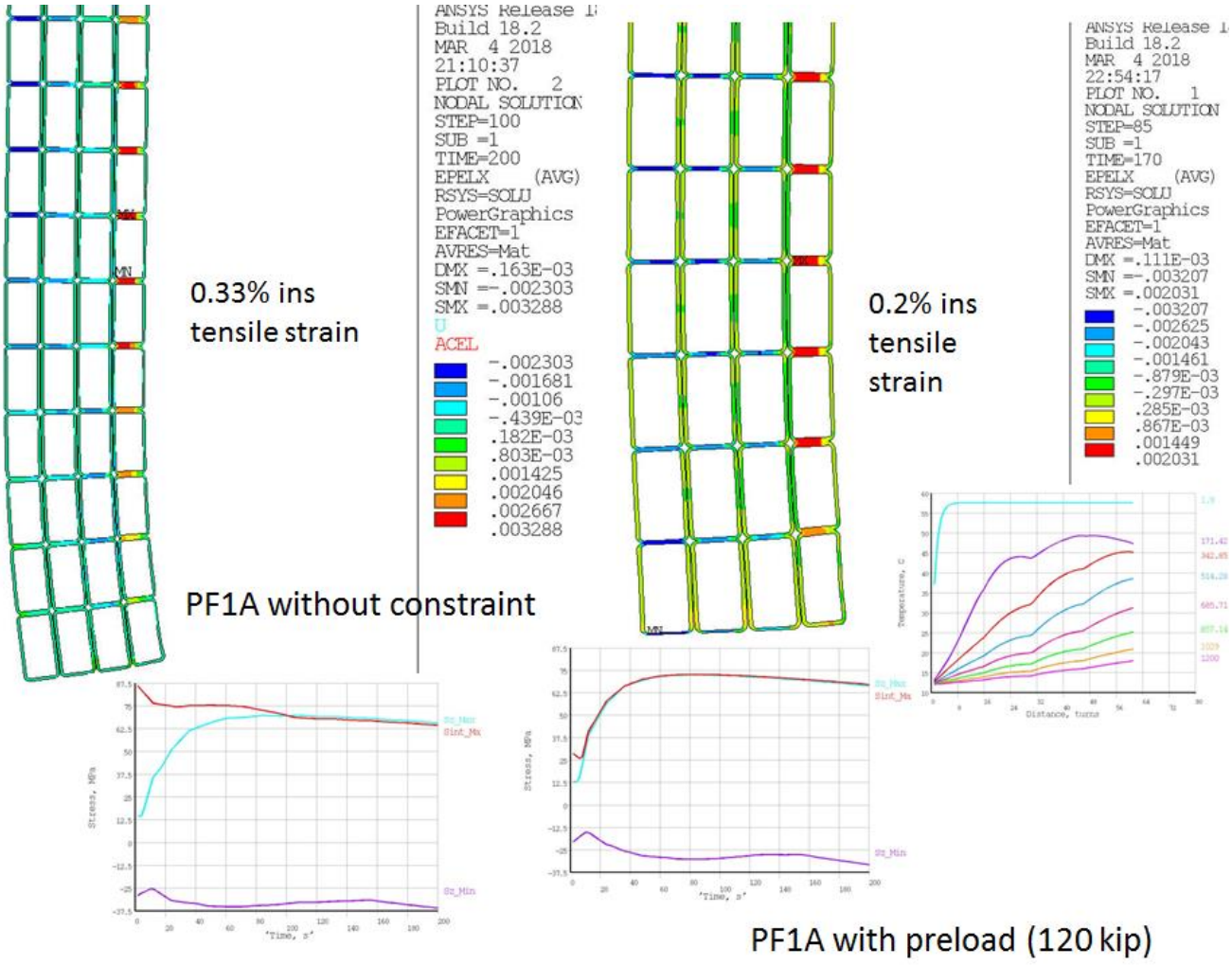

Figure 15 PF-1a - Insulation tensile strain (0.3% no pre-load - left) and (0.2% with pre-load – right) (Low insulation modulus)

Table 9 – Sensitivity Study (factor of 2 variation on insulation property)

Impact of Insulation property to	Mass density	Thermal conductivity	Elastic modulus	Coefficient of thermal expansion
Conductor stress	**5-7%**	**15%**	**5%**	**~6%**
Insulation strain			**50%**	**>20%**
Interface pre-loads	**<5%**	**3-5%**	**30%**	**>20%**

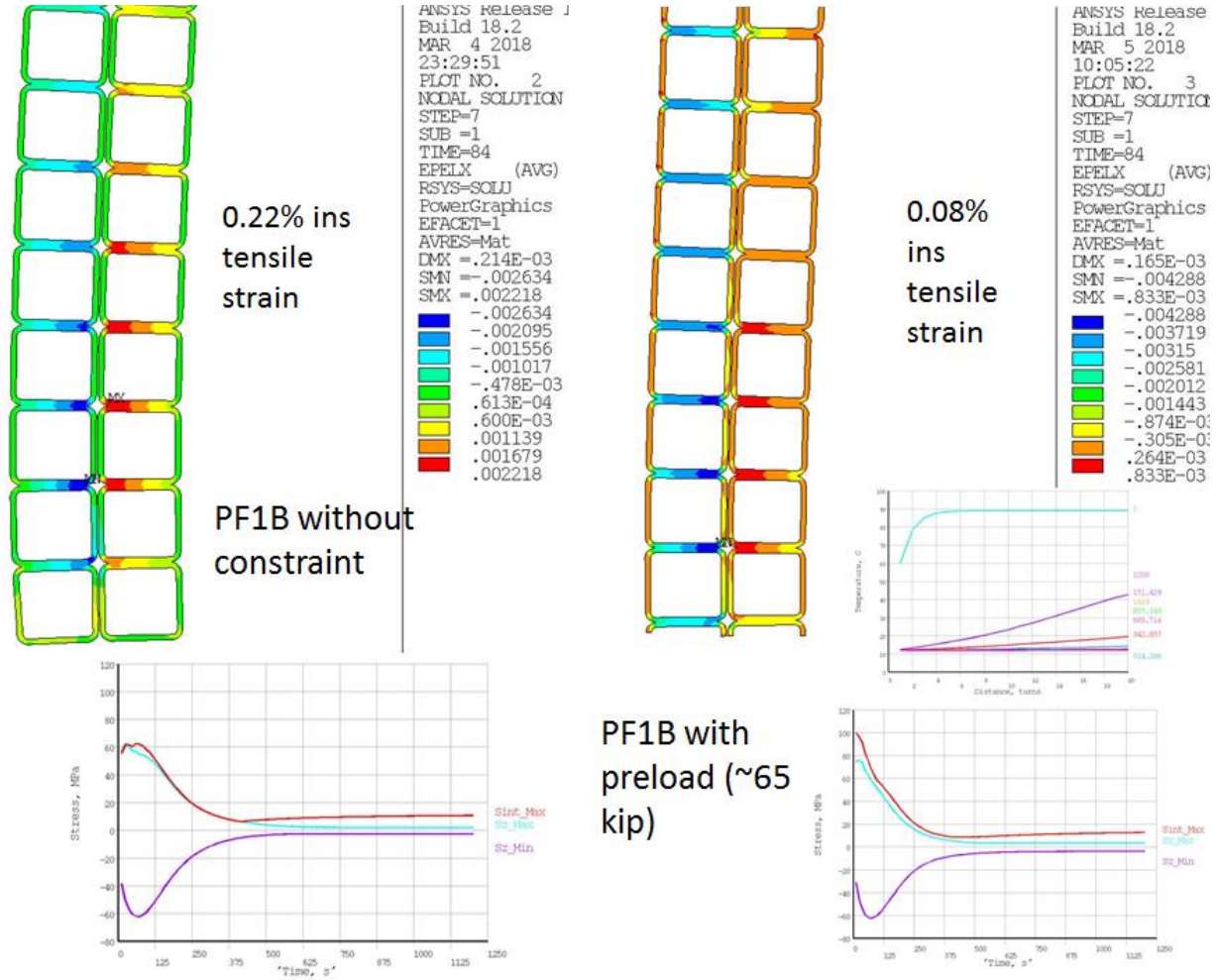

Figure 16 PF-1b - Insulation tensile strain (0.22% no pre-load - left) and (0.08% when pre-loaded – right) (Low insulation modulus)

PF-1a Conductor Dimension and Cooling Hole Size

The present evaluation of coil conductor modifications is largely based on the maximum temperature at the end of pulse and the maximum thermal stress due to a temperature gradient during cool down of inner PFs. The acceptance of the conductor modification is largely driven by meeting the 1200 sec repetition period requirement and the conductor fatigue crack propagation requirement [1, 6]. Figure 17 below presented the comparison of the PF1A conductor size (top) and transient cool down along the coil winding (inlet to outlet) (bottom) between the inner PF PDR design (left) and the modifications at the conductor size peer review (right). The same thickness of ~3.75 mm from the side of the hole to the side edge of PF-1a conductor is well maintained under this proposed modification as shown on the top panel in Figure 17 without compromise the fatigue crack propagation requirement [8].

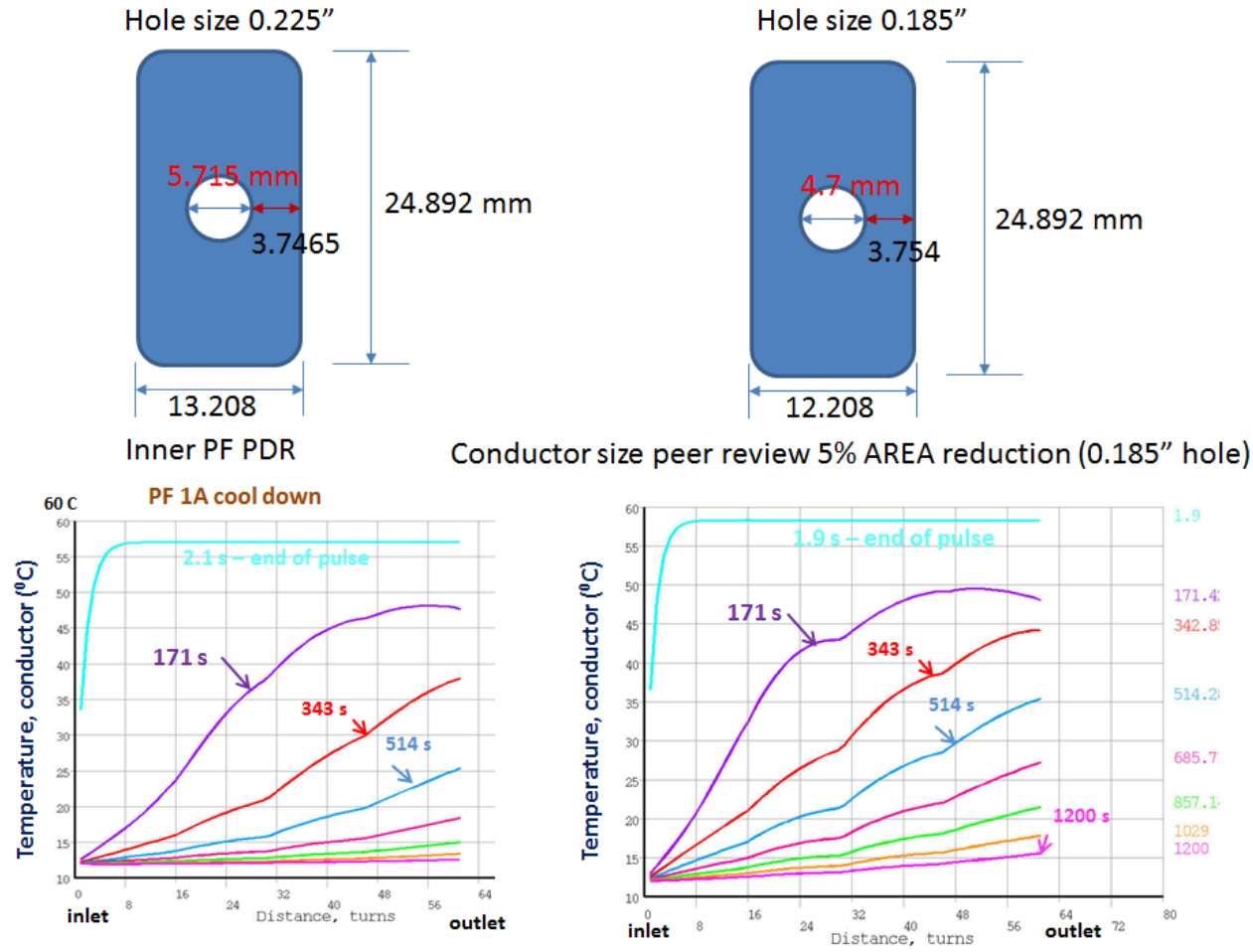

Figure 17 PF1b Comparison (PDR design vs conductor size peer review) of max temperature at end of pulse and end of cool down from the 2D transient thermal analysis

Table 10 Maximum temperature at the end of pulse and end of cool down

	Inner PF PDR	Conductor size peer review
End of pulse	58 ^{0}C	58.44 ^{0}C
End of cool down	12.8 ^{0}C	16 ^{0}C

To confirm that little ratcheting is expected for the conductor modifications as a result of the 3-4 degrees higher than nominal inlet water temperature, a 1200 sec repetition of the transient thermal analysis for three pulses was performed to quantify the level of temperature change at the end of the 3 pulse repetition. The temperature difference at the outlet between end of first pulse and the third pulse is only <0.2 ^{0}C and little change in the maximum conductor stress is expected (Figures 18-19).

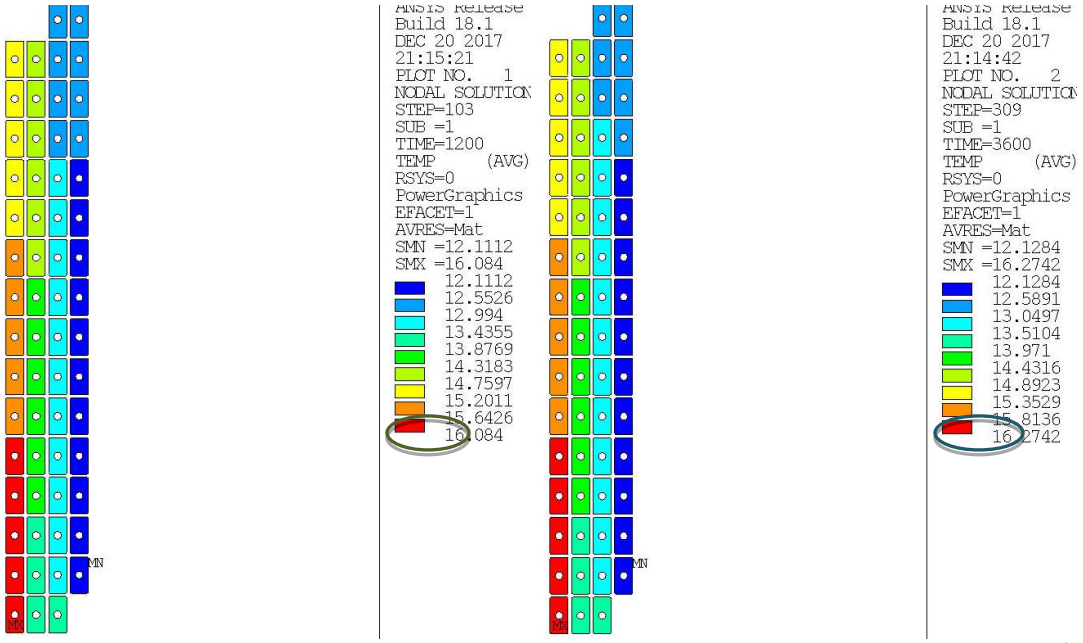

Figure 18 PF1b Comparison max temperature at end of cool down between 1st pulse (left, 16 C) and 3rd pulse (right 16.2 C, only 0.19 C increase of max temperature)

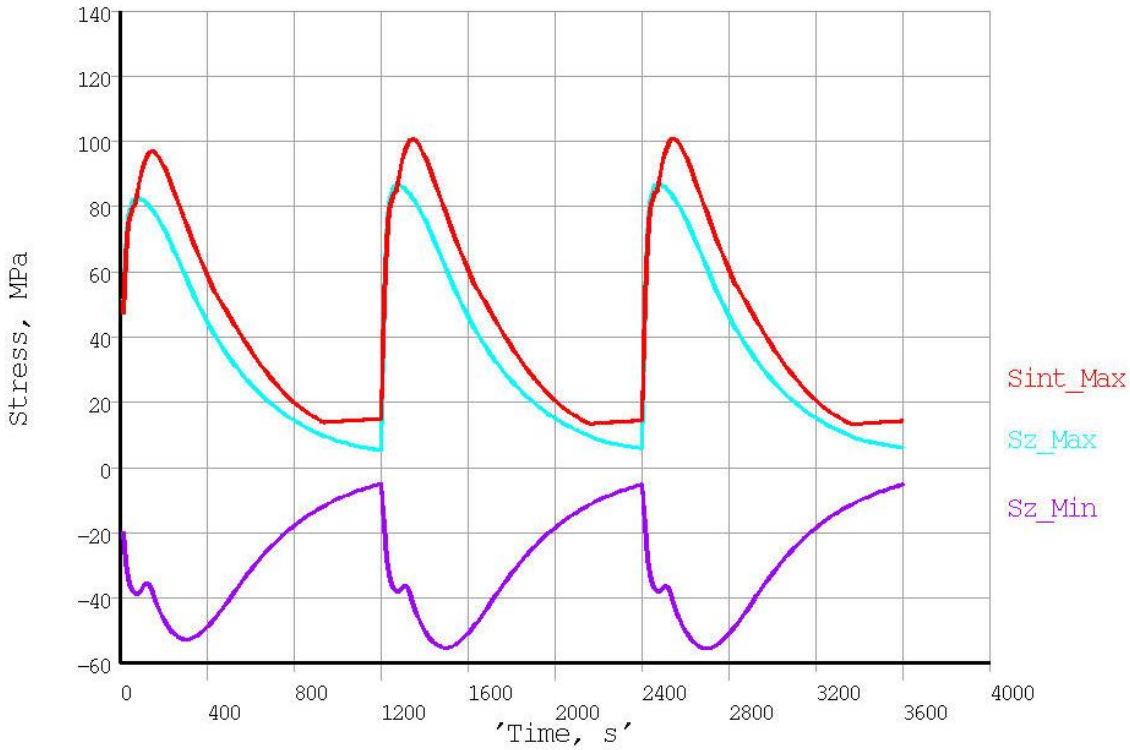

Figure 19 Transient thermal stresses during cool down from 1st pulse to 3rd pulse, <5% ratcheting and stress is settling down at the 3rd thermal cycle

Conclusion: *(Specify whether or not the purpose of the calculation was accomplished)*

Transient thermal analyses were performed for the inner PF coils PF-1a, -1b and -1c using 2D axis-symmetric models developed with fluid-solid coupled solving capability. Flow rates are based on available pressure drop 400 psi and the pump is assumed to deliver constant pressure while not limited to the flow, which varies with temperature due to large variation in the fluid viscosity. The FDR thermal analysis is based on the new physics requirements [2] and the latest coil design parameters [3] including PF-1a conductor size modifications [6] with suggested cross section area reduction to provide positional adjustment capability.

The main conclusions include

1. *The conductor static and fatigue stresses meet the NSTX-U structural design limits. The insulation shear and compressive stresses meet the design allowable but pre-load is required to limit and minimize the insulation normal tensile strain.*

2. *The sensitivity study showed that uncertainty in insulation elastic modulus (a factor of 3) will increase the insulation tensile strain from ~0.1s% to ~0.2s% (the maximum is on PF-1a). The recommendation is to ensure insulation system to reach high elastic modulus as high as achievable so to minimize impact to coil structural integrity.*

3. *There is 0.4 ^{0}C peak temperature increase with the 5% area reduction for 1A and 10% ESW reduction compared to the inner PF PDR design. There is also a 3 ^{0}C increase of peak temperature in water outlet at end of cool down*.

4. *Additional analysis of 1200 sec repetition for 3 pulses shows that very little ratcheting on the temperature and conductor stress is expected with the proposed modifications.*

5. *Additional ESW reduction (13-15%) may fully eliminate the concern of this slight temperature increase at end of 1200 sec cool down period.*

Considering the operational fact that maximum full current and full pulse length won't happen at the same time (full current operation is likely to happen with less than full pulse length), the PF-1a conductor modification may be acceptable with limited risks. The full evaluation of conductor and insulation stress and strain is completed for the Final Design Review of the inner PF coils.